Nuclear Instruments and Methods in Physics Research A ∎ (∎∎∎∎) ∎∎∎–∎∎∎

Contents lists available at ScienceDirect

Nuclear Instruments and Methods in Physics Research A

journal homepage: www.elsevier.com/locate/nima

Modeling and simulation of charge collection properties for 3D-trench electrode detector

Hao Ding [a,b], Jianwei Chen [a,b], Zheng Li [a,b,c,*], Shaoan Yan [a,b]

[a] School of Materials Science and Engineering, Xiangtan University, Xiangtan 411105, China
[b] Center for Semiconductor Particle and photon Imaging Detector Development and Fabrication, Xiangtan University, Xiangtan 411105, China
[c] Brookhaven National Laboratory, Upton, NY, USA[1]

ARTICLE INFO

Keywords:
3D-trench electrode detectors
Device simulation
Induced current
Charge collection property

ABSTRACT

3D-trench electrode detectors were simulated in this paper. Charge collection of 3D-trench electrode detector was simulated using the full 3D device simulation. The induced current and collected charge caused by drifting carriers, generated by a minimum ionizing particle (MIP) incident through the detector, have been modeled and calculated. The results indicate that the total collected charge in irradiated detector change with particle incident position and radiation fluence. In addition, we have estimated the average total collected charge generated by a MIP incident in 3D-trench electrode detector.

1. Introduction

For silicon detector applications in the extremely harsh radiation environments, for example, the Large Hadron Collider (LHC), or the upgrade of the LHC at CERN, the total radiation fluence can reach up to 1×10^{16} n_{eq}/cm^2, leading to severe degradations in detector performance [1]. One of the technologies to enhance the radiation tolerance of detectors is by detector structure engineering with novel detector structures. Among them, the 3D silicon detectors get much attention because of their many advantages, such as much lesser charge trapping and much lower full depletion voltage than those of the planar detectors. 3D detectors were first proposed by Parker et al. [2–3] in the middle 90s, as shown in Fig. 1, which is the conventional 3D electrode detector with all column electrodes penetrating through the silicon substrate. In recent years, a number of variants of the conventional 3D electrode detectors have emerged [2–7], including single or double-type-column [6], and one or double-sided 3D detectors [7], whose electrodes are all in the shape of column. The electric fields in these conventional 3D detectors are non-uniform, and very high electric fields exist near the junction column. Recently, a new 3D-trench electrode detector has been proposed. In this new 3D-trench electrode configuration detector, the outer electrodes are etched as trenches deep into the Si bulk, and the inner electrodes are normally etched columns (although sometimes they also can be trenches) deep into Si bulk. This new 3D-trench electrode detector has more uniform electric field and lower depletion voltage than those in conventional 3D detectors [8]. Because of these advantages, the charge collection properties of 3D-trench electrode detectors will be at least the same, if not more than, as those of conventional 3D detectors.

In this article, we will report the charge collection simulation of the 3D-trench electrode detector. This will be done through the 3D device simulation on the 3D-trench electrode detector and modeling of the charge collection generated by a MIP incident vertically through the detector. We will discuss the effect of charge collection on the 3D-trench electrode detector with various MIP incident positions and various radiation fluences.

2. Simulation and device description

Full 3D TCAD simulations on a 3D-trench Si detector were performed using the DEVICE3D package of ATLAS Silvaco [9]. The electric field and the weighting field of detectors are obtained from simulation (as shown in Fig. 3). As shown in Fig. 2, depths of the n^+ trench electrode and the p^+ column electrode are 270 μm, extenting into the 300 μm thick p-type Si bulk. Widths of the outer trench electrode and the central column electrode are 10 μm. The edge length of the trench electrode is 100 μm. The n^+ trench electrode and the p^+ column electrode are covered by aluminum layers on the detector surface, and other areas of detector surface are covered by a silicon oxide layer. The backside of detector is not processed, and it is only covered by a uniform silicon oxide layer. The oxide charge density is 4×10^{11} cm^{-2} for both sides. The initial doping concentration of p-type bulk is 1×10^{12} cm^{-3}. For severely irradiated detectors ($\Phi>1\times10^{14}$ n_{eq}/cm^2), one of the most important radiation effects in the detector is space charge transformation. Here, we use the doping concentration to simulate the space charge induced by

[1] Before 01.07.14.

* Corresponding author at: School of Materials Science and Engineering, Xiangtan University, Xiangtan, 411105, China.
E-mail address: zhengli58@gmail.com (Z. Li).

http://dx.doi.org/10.1016/j.nima.2015.04.065
0168-9002/

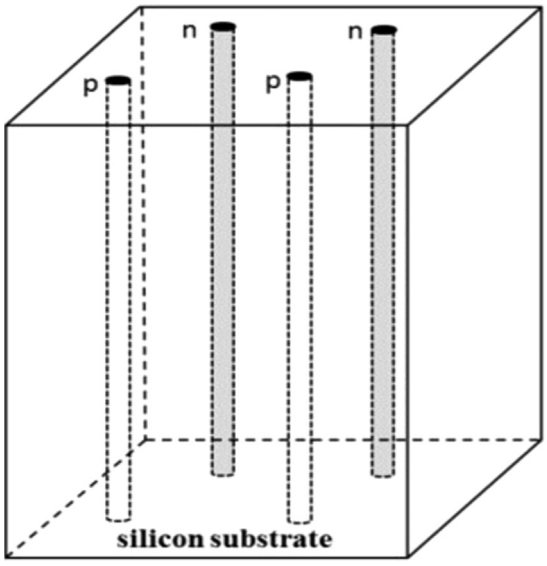

Fig. 1. Illustration of a conventional 3D-delectrode Si detector.

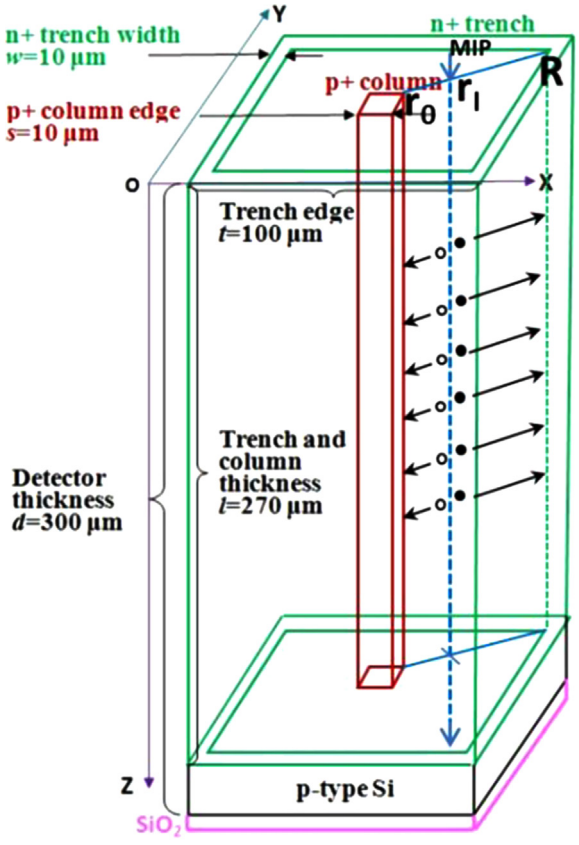

Fig. 2. A Schematic of a MIP incident in the simulated square 3D-trench electrode detector.

radiation effects, which will achieve the main effect of space charge change by irradiation induced space charge changes. This is only an approximation that cannot account for secondary effects caused by actual deep levels, such as temperature dependence. We note that no defect model was used to account to some new effects, such as the double junction effect, etc., which should however, significantly change the physics result here [12,14]. According to the empirical model, the effective doping concentration, N_{eff}, can be represented as the function of radiation fluence, as (for N-type Si):

$$N_{eff} \cong N_{d0} e^{-\gamma \Phi_{eq}} - \beta \Phi_{eq}. \quad (1)$$

where N_{d0} is the initial doping concentration, γ the donor removal rate, and β the introduction rate for deep acceptors, $\Phi_{eq}$is the 1-MeV neutron-equivalent fluence [10–13]. The first term in Eq. (1) is the donor removal, and the second term acceptor creation. Since γ is about 1×10^{-13} cm^2 and β here is 0.01/cm for protons radiation [12],

$$\text{for } \Phi_{eq} > 1 \times 10^{14} \mathrm{n}_{eq}/\mathrm{cm}^2,\ N_{eff} \cong -\beta \Phi_{eq}. \quad (2)$$

Similarly, the boron removal effect can be neglected for $\Phi_{eq} > 1 \times 10^{14}$ n$_{eq}$/cm^2.

The full device was simulated, including the top surface (z=0 μm) and the region near bottom surface (z=300 μm), which are 3D boundary conditions. Also square shape gives a 3D asymmetry. All of these cannot be simulated by a simple 2D simulation. However, in our paper, only the bulk electric field and charge collection properties will be given, which are data from a series of 2D cuts from the full 3D data. Electric field along the top surface is quite non-uniform due to surface charges, but the depth of this non uniformity is only in the order of 10–20 μm. The electric field near the bottom is now as high as that at the top (not relevant for surface breakdown considerations), but still high enough for effective charge collection.

3. Induced current

To simplify the charge collection model, assuming a MIP incident through the detector from the front side to the backside vertically (as shown in Fig. 2), the number of electron–hole pairs generated along the particle's track is q=80 e's/μm. The incident position of a MIP, r_I, is selected at the diagonal of detector surface, from r_0 to R. In this case (θ=45°), the electric field is the lowest (shown in Fig. 3), so it has the most heavily charge trapping effect for drifting carriers, and the charge collection ability is the weakest. Our calculation gives the lower limit of the charge collection for the structure (square shape here), which is important to the practical applications. The other extreme is at θ=0°, which is the higher limit, and the charge collection at θ=45° is only about 10–20% lower than that at θ=0°.

According to Ramo Theorem, the induced current for electrons and holes at t time is [15]:

$$i^{e,h}_{r_I}(t) = q_{e,h} \cdot v^{e,h}_{dr} \cdot E_w \quad (3)$$

where the charge for electrons or holes $q_{e,h} = 80\ e's/\mu m \times d_{eff}$, $v^{e,h}_{dr}$is the drift velocity for electrons and holes, E_w is the weighting field, obtained from 3D simulation, andd_{eff} (=270 μm here), is the effective depth of detector and it is the depth of the trench electrode. The drift velocity $v^{e,h}_{dr}$ for electrons or holes, taking into account the saturation velocity, v$_s$, can be expressed as:

$$v^{e,h}_{dr} = \frac{dr^{e,h}}{dt} = \frac{u^{e,h} E(r^{e,h})}{1 + \frac{u^{e,h} E(r^{e,h})}{v_s}} \quad (4)$$

here v_s is about 1×10^7 cm/s as approximation for both electrons and holes, where$u^{e,h}$is the carrier's low field mobility for holes or electrons(1450 cm^2/s/V for electrons and 450 cm^2/s/V for holes), $r^{e,h}$ is the position of drifting electron or hole, and $E(r^{e,h})$(obtained from 3D simulation) is the electric field in the detector at position $r^{e,h}$.

Considering boundary conditions:

$$\begin{cases} r^e(t=0) = r_I, \quad r^e(t=t^e_{dr}) = R \\ r^h(t=0) = r_I, \quad r^h(t=t^h_{dr}) = r_0 \end{cases} \quad (5)$$

Eqs. (4) and (5) can be solved numerically to obtain:

$$\begin{cases} r^{e,h} = r^{e,h}(t, r_I, t^{e,h}_{dr}) \\ t^e_{dr} = t^e_{dr}(r_I, R), \quad t^h_{dr} = t^h_{dr}(r_I, r_0) \end{cases} \quad (6)$$

where $t^{e,h}_{dr}$ is total transient time for electrons or holes. The induced